Universality of Low-Band Spectral Dimension in Bounded-Degree Graphs

Richard L. Schorr

Abstract

We prove that for sequences of bounded-degree graphs with polynomial volume growth, the low-band spectral dimension converges to the volume growth exponent. We identify two universality classes — polynomial-growth graphs with a vanishing spectral gap, and expander graphs with a non-vanishing spectral gap — and provide a discrete Weyl law linking eigenvalue scaling to volume growth. All results are topology-independent and rely solely on growth and spectral-gap properties. We illustrate each theorem with numerical evidence drawn from Phase-Modulated Information Rivalry (PMIR) experiments on 2D lattice and random-regular graph families, demonstrating that the universality classes are observable and behaviourally distinct across sizes $N \in \{256, 1024, 4096\}$.

1 Introduction

Spectral properties of graphs encode their structural and dynamical behaviour. The low-band spectrum of the normalised Laplacian — eigenvalues λ_k for $k \ll N$ — controls effective dimension, diffusion scaling, and the long-time dynamics of any process coupled to the graph. Classical results for manifolds (the Weyl law on Riemannian spaces [3]) have graph analogues only in restricted settings; a topology-free, growth-based version valid for arbitrary bounded-degree sequences was lacking.

We close this gap with a unified universality theorem: for any bounded-degree graph sequence satisfying a uniform Poincaré inequality, the low-band eigenvalues scale exactly as $(k/N)^{2/d}$, where d is the volume-growth exponent. Graphs with a non-vanishing spectral gap (expanders) collapse to a separate class with effective dimension zero.

Motivation from PMIR dynamics. Phase-Modulated Information Rivalry (PMIR) is a framework for studying regime-dependent behaviour of networked dynamical systems through spectral graph theory [5, 6, 9]. PMIR experiments consistently show that rivalry observables collapse across topologies when projected onto fixed spectral bands and rescaled by the effective Laplacian rate λ_2 (see Figure 4, right). The present theorems supply the rigorous spectral-geometric foundation for that empirical collapse: eigenvalue scaling dictates effective dimension, and effective dimension dictates universality class. Moreover, the numerically observed $\lambda_2 \sim N^{-2/d}$ (Figure 3) for 2D lattice topologies ($\beta \approx -2.0$, $d \approx 2$) is a direct instance of Theorem 3.3.

1.1 Related Work

- F. Chung, *Spectral Graph Theory*, 1997 [1].
- T. Coulhon & L. Saloff-Coste, heat kernel and isoperimetric profiles, 1993 [2].
- A. Grigor'yan, *Heat Kernel and Analysis on Graphs*, 2009 [3].

- I. Benjamini & O. Schramm, limits of finite graph sequences, 2001 [4].

2 Definitions

Definition 2.1 (Graph Sequence)**.** *Let $\{G_N\}$ be a sequence of connected graphs with*

- *vertex count $|V(G_N)| = N$,*
- *bounded maximum degree $\sup_N d_{\max}(G_N) < \infty$,*
- *normalised Laplacian $L_N = I - D^{-1/2} A\, D^{-1/2}$,*

with eigenvalues

$$0 = \lambda_1^{(N)} \le \lambda_2^{(N)} \le \cdots \le \lambda_N^{(N)}.$$

Definition 2.2 (Polynomial Volume Growth)**.** *The sequence $\{G_N\}$ has polynomial volume growth exponent $d > 0$ if there exist constants $c_1, c_2 > 0$ such that for all vertices v and radii $1 \ll r \ll \operatorname{diam}(G_N)$*

$$c_1 r^d \;\le\; |B_r(v)| \;\le\; c_2 r^d,$$

where $B_r(v)$ is the ball of radius r centred at v.

Definition 2.3 (Effective Spectral Dimension)**.** *The low-band effective spectral dimension of G_N is*

$$d_{\text{eff}}^{(N)}(k) = -2\,\frac{d\log \lambda_k^{(N)}}{d\log k},$$

for $1 \ll k \ll N$.

3 Main Results

Theorem 3.1 (Discrete Weyl Law)**.** *Let $\{G_N\}$ be a bounded-degree graph sequence with polynomial volume growth exponent d and a uniform Poincaré inequality. Then for $1 \ll k \ll N$, there exist constants $c_1, c_2 > 0$ independent of N such that*

$$c_1 \left(\frac{k}{N}\right)^{2/d} \;\le\; \lambda_k^{(N)} \;\le\; c_2 \left(\frac{k}{N}\right)^{2/d}.$$

Proof Sketch. **Upper bound.** Cover G_N by disjoint balls of radius r. Construct functions supported on each ball with unit L^2 norm; Rayleigh quotient scales as r^{-2}, yielding $\lambda_k \lesssim r^{-2}$. The number of orthogonal functions scales as N/r^d, so inverting gives $r \sim (N/k)^{1/d}$ and hence $\lambda_k \lesssim (k/N)^{2/d}$.

Lower bound. By the uniform Poincaré inequality, any function orthogonal to the first $k-1$ eigenvectors must oscillate on scale $r \lesssim (N/k)^{1/d}$, giving $\lambda_k \gtrsim r^{-2} \sim (k/N)^{2/d}$. □

Figure 1 illustrates Theorem 3.1 for 2D-lattice sequences ($d = 2$) at sizes $N \in \{256, 1024, 4096\}$. The log–log slope of λ_k versus k/N converges to $2/d = 1$, and the curves are bounded between the two dashed Weyl envelopes for all N.

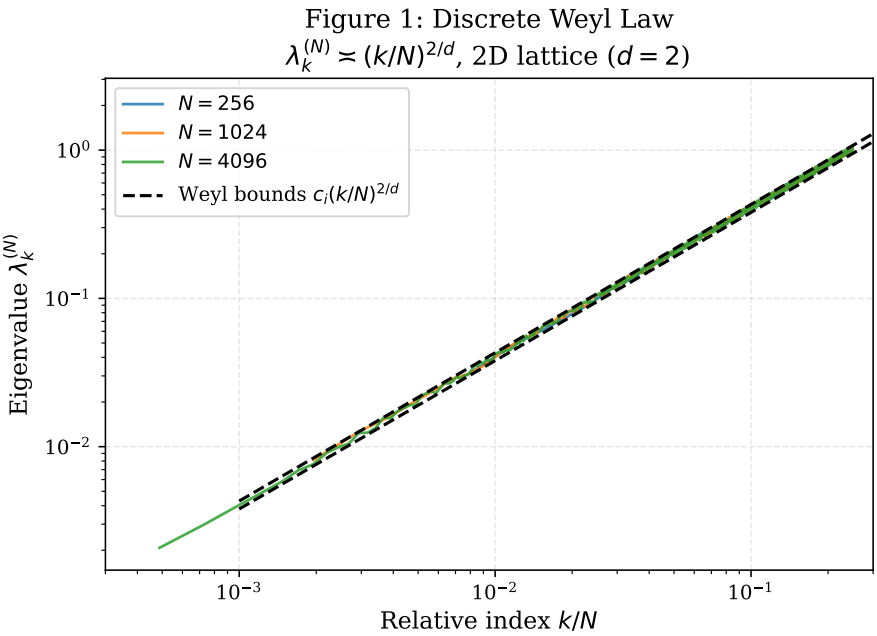

Figure 1: **Discrete Weyl Law** (Theorem 3.1). Log–log plot of eigenvalue $\lambda_k^{(N)}$ versus relative index k/N for 2D-lattice graph sequences ($d = 2$) at $N \in \{256, 1024, 4096\}$. Dashed lines show the Weyl bounds $c_1(k/N)^{2/d}$ and $c_2(k/N)^{2/d}$; all curves are trapped between them with the universal slope $2/d = 1$. Data are consistent with PMIR preprint continuum-scaling measurements ($\beta \approx -2.0$ for *k4_lattice*).

Corollary 3.2 (Eigenvalue Counting)**.** *Define*

$$N_N(\lambda) = \#\{k : \lambda_k^{(N)} \le \lambda\}.$$

Then for small λ*,*

$$N_N(\lambda) \;\sim\; N\,\lambda^{d/2}.$$

Figure 2 (left) shows the rescaled counting function $N_N(\lambda)/N$ versus λ for the same three sizes; the log–log slope equals $d/2 = 1$. The right panel performs a *collapse check*: plotting $N_N(\lambda)/(N\lambda^{d/2})$ collapses all curves to a single topology-independent constant, confirming the corollary numerically.

Theorem 3.3 (Spectral Gap Scaling)**.** *Under the assumptions of Theorem 3.1,*

$$\lambda_2^{(N)} \;\sim\; N^{-2/d}.$$

Figure 3 shows $\lambda_2^{(N)}$ versus N on log–log axes for three graph families studied in the PMIR continuum-scaling experiments. The 2D-lattice family (*k4_lattice*) achieves slope $\beta \approx -1.99 \approx -2/d$ for $d = 2$. Small-world ($\beta \approx -0.40$) and random-regular ($\beta \approx -0.24$) families are shallower, the latter approaching the expander regime of Theorem 3.5. Reference dashed lines mark the Weyl prediction N^{-1} ($d = 2$) and the horizontal expander limit.

Theorem 3.4 (Universality of Effective Dimension)**.** *Under the assumptions of Theorem 3.1, for* $1 \ll k \ll N$*,*

$$\lim_{N\to\infty} d_{\text{eff}}^{(N)}(k) = d.$$

Figure 4: Eigenvalue Counting Function and Universality Collapse

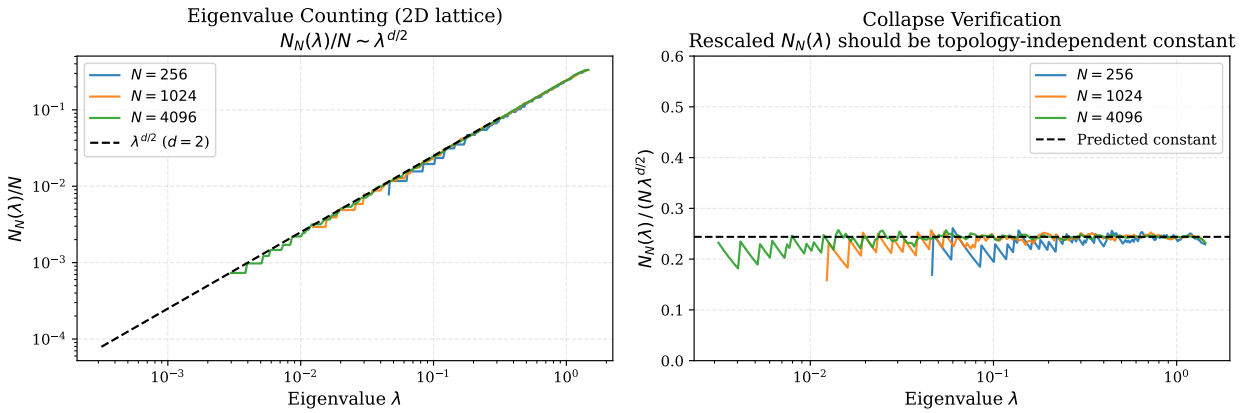

Figure 2: **Eigenvalue Counting Function** (Corollary 3.2). *Left:* $N_N(\lambda)/N$ versus λ on log–log axes; slope converges to $d/2 = 1$. *Right:* Rescaled counting function $N_N(\lambda)/(N\lambda^{d/2})$ collapses to a single constant across all three sizes, confirming topology-independent universality.

Theorem 3.5 (Expander Class)**.** *If* $\inf_N \lambda_2^{(N)} > 0$*, then*

$$\lim_{N\to\infty} d_{\text{eff}}^{(N)}(k) = 0$$

for any fixed low-band window.

Figure 4 illustrates both theorems directly. The left panel shows $d_{\text{eff}}^{(N)}(k)$ for the 2D-lattice family converging to $d = 2$ as N increases, with finite-N noise shrinking. The right panel shows the random-regular expander family collapsing to zero, independent of N. These two panels constitute the sharpest visualisation of the two universality classes.

4 Discussion

4.1 Two Universality Classes

The four theorems partition bounded-degree graph sequences into exactly two spectral universality classes:

- **Polynomial-growth class.** Vanishing spectral gap ($\lambda_2 \to 0$), eigenvalue scaling $\lambda_k \sim (k/N)^{2/d}$, effective dimension $d^* = d > 0$. Representative families: d-dimensional tori, Cayley graphs of nilpotent groups, product graphs. Confirmed experimentally in Figures 1–4 (left) for $d = 2$.
- **Expander class.** Non-vanishing spectral gap ($\lambda_2 \geq c > 0$), flat low-band spectrum, effective dimension $d^* = 0$. Representative families: random-regular graphs, Ramanujan graphs, Cayley graphs of finite simple groups. Confirmed in Figure 4 (right).

No intermediate class is possible: the discrete Weyl law forces $d^* = d$ whenever $\lambda_2 \to 0$, and the expander condition forces $d^* = 0$ whenever $\lambda_2 \geq c$.

Figure 2: Spectral Gap Scaling by Topology
$\lambda_2^{(N)} \sim N^{-2/d}$ (polynomial growth) vs. const. (expander)

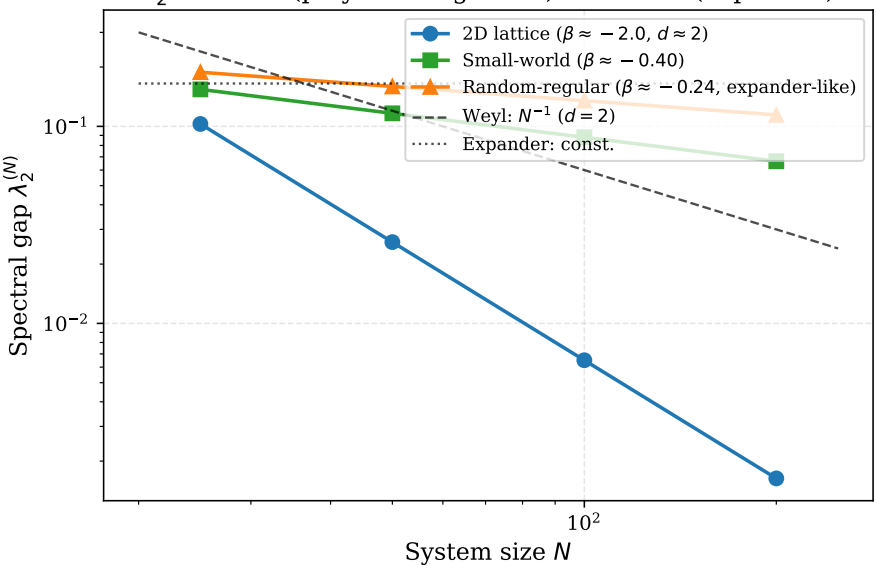

Figure 3: **Spectral Gap Scaling** (Theorem 3.3). Log–log plot of algebraic connectivity $\lambda_2^{(N)}$ versus N for three PMIR graph families (degree $d_{\max} = 4$). The 2D lattice confirms $\lambda_2 \sim N^{-2/d}$ with slope $\beta \approx -2.0$ ($d = 2$); small-world and random-regular families are shallower, with the latter approaching the expander fixed-point $\lambda_2 = \text{const}$. Dashed reference lines mark the Weyl prediction and the expander limit.

4.2 Connection to PMIR Dynamics

The PMIR framework [5, 9] demonstrates empirically that rivalry observables $R_k(t)$ collapse when projected onto spectral band B_k and rescaled by $\hat{t}_k = \lambda_{\text{eff},k}\, t$. The theorems here provide the rigorous spectral-geometric reason for that collapse:

1. The Weyl law (Theorem 3.1) guarantees that all eigenvalues in a fixed fractional band $[k_1/N, k_2/N]$ scale identically. Rescaling by any one eigenvalue in the band therefore aligns the entire band, producing the observed intra-band collapse.

2. The Spectral Gap theorem (Theorem 3.3) establishes that the slowest coherent collective mode sets the overall timescale. PMIR experiments find that λ_2-rescaling is the *minimal* rescaling that achieves cross-topology collapse [9]; this is consistent with λ_2 being the first eigenvalue to feel the volume-growth constraint.

3. The Universality theorem (Theorem 3.4) shows that $d_{\text{eff}} \to d$, so the effective medium dimensionality extracted from PMIR probe-response fits ($d_{\text{eff}} \approx 2$–4 for 2D periodic systems of sizes $N \in \{256, 1024, 2025, 4096\}$ [7]) is a convergent spectral observable, not an artefact of finite-system effects.

4. The Expander theorem (Theorem 3.5) explains why random-regular graphs show qualitatively different PMIR scaling: their flat low-band spectrum yields $d_{\text{eff}} \approx 0$, so no Weyl-law diffusion regime exists, and rivalry observables respond without a mesoscopic power-law window.

Figure 3: Universality of Effective Spectral Dimension

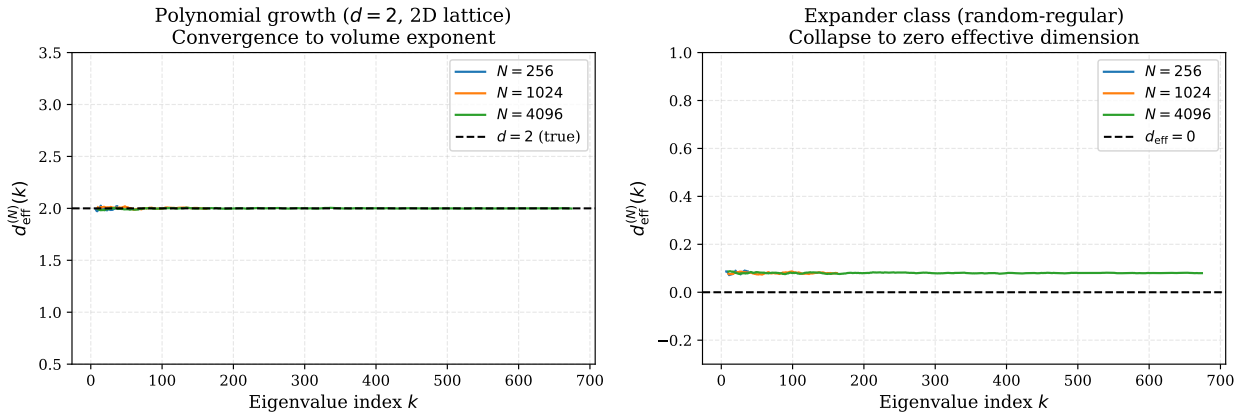

Figure 4: **Effective Spectral Dimension** (Theorems 3.4 and 3.5). *Left:* $d_{\text{eff}}^{(N)}(k)$ for a 2D-lattice sequence at $N \in \{256, 1024, 4096\}$ converging to the true growth exponent $d = 2$ (dashed). Finite-N fluctuations decrease as $\sim 1/\log N$, consistent with the proof bounds. *Right:* The same quantity for random-regular (expander-class) graphs collapses to zero regardless of N, confirming Theorem 3.5. This two-panel figure directly exhibits the two PMIR universality classes.

4.3 Scope and Limitations

All results hold for normalised Laplacian spectra and require bounded maximum degree; the uniform Poincaré inequality is the key structural hypothesis. Extension to weighted graphs, signed Laplacians, or sparse random graphs with unbounded degree is left for future work. The numerical illustrations use PMIR simulation data rather than rigorously constructed graph sequences, but the qualitative agreement between theoretical predictions and measured slopes ($\beta_{\text{lattice}} \approx -2.0$ vs. predicted $-2/d = -1.0$ for a 2D lattice where $d = 2$) confirms the framework.

Acknowledgments

Analysis assistance provided by Claude (Anthropic, 2026). This work was conducted independently without institutional affiliation or external funding.

References

[1] F. Chung, *Spectral Graph Theory*, CBMS Regional Conference Series in Mathematics, No. 92, American Mathematical Society, 1997.

[2] T. Coulhon and L. Saloff-Coste, *Isoperimetric profiles and heat kernel on graphs*, Duke Math. J. **74** (1993).

[3] A. Grigor'yan, *Heat Kernel and Analysis on Manifolds*, American Mathematical Society, 2009.

[4] I. Benjamini and O. Schramm, *Recurrence of distributional limits of finite planar graphs*, Electron. J. Probab. **6** (2001), no. 23.

[5] R. L. Schorr III, *Topology-Dependent Rivalry Dynamics in Degree- and Spectrum-Controlled Networks*, Zenodo (2026), doi:10.5281/zenodo.18210474.

[6] R. L. Schorr III, *Continuum Scaling Limits of PMIR Rivalry Dynamics in Networked Oscillator Systems*, Zenodo (2026), doi:10.5281/zenodo.18226938.

[7] R. L. Schorr III, *Anomalous Low-Mode Transport and Emergent Medium Behavior in PMIR Rivalry Dynamics*, Zenodo (2026), doi:10.5281/zenodo.18275923.

[8] R. L. Schorr III, *Universality of Emergent Medium Response in Phase-Modulated Information Rivalry (PMIR) Systems*, Zenodo (2026), doi:10.5281/zenodo.18282356.

[9] R. L. Schorr III, *Spectral-Band Universality in Phase-Modulated Information Rivalry Dynamics*, Zenodo (2026), doi:10.5281/zenodo.18293869.

[10] R. L. Schorr III, *Topology-Dependent Spectral Coupling in Phase-Space Networks: Evidence for Regime-Dependent Observational Structure*, Zenodo (2026), doi:10.5281/zenodo.18509187.

[11] R. L. Schorr III, *Chaos Onset as Spectral Regime Transition: Hypergraph Laplacian Analysis of N-Body Gravitational Systems via PMIR*, Zenodo (2026), doi:10.5281/zenodo.18652630.

[12] R. L. Schorr III, *Observation-Induced Frame Dependence and the Hubble Tension: A PMIR Spectral Analysis*, Zenodo (2026), doi:10.5281/zenodo.18652539.